Measurement and Analysis of Junction Temperature of Semiconductor Laser Devices

Yang Yang[1,2] Yu Guolei[1,2] Li Peixu[2] Xia Wei[2] Xu Xiangang[1,2]

[1]*State Key Laboratory of Crystal Material, Shandong University, Jinan, Shandong* 250100, *China*

[2]*Shandong Huaguang Optoelectronics Co. Ltd, Jinan, Shandong* 250100, *China*

Abstract Junction temperature/thermal-resistance is reflected in the comprehensive cooling capacity of laser devices, which is closely related to the sintering quality of the solder layer. The operating junction temperatures of laser devices have been detected by the forward-voltage and wavelength-shift methods. The distribution of voids in the solder layer have been analyzed using a scanning acoustic microscope. The results verify the feasibility of junction temperature measurement, and confirm the relation between the junction temperature and the sintering quality of laser chips. These results will pave the way for the development of semiconductor lasers and the filtering of laser devices.

Key words lasers; junction-temperature; thermal-resistance; scanning acoustic microscope

OCIS codes 120.6780; 140.5960; 140.6810

半导体激光器结温的测试及分析

杨 扬[1,2] 于果蕾[1,2] 李沛旭[2] 夏 伟[2] 徐现刚[1,2]

[1]山东大学晶体材料国家重点实验室, 山东 济南 250100

[2]山东华光光电子有限公司, 山东 济南 250100

摘要 结温/热阻是反映激光器器件散热能力的综合参数,与封装焊料层的烧结质量关系密切。本文分别通过正向电压法和波长漂移法,测试计算得到激光器的工作结温,利用扫描声学显微镜分析了激光器焊料层中空洞分布;验证了结温测试方法的可行性,并确认了激光器结温与焊料层烧结质量之间的对应关系,相关结果将指导半导体激光器的研制改进和器件分筛。

关键词 激光器; 结温; 热阻; 扫描声学显微镜

中图分类号 TN248 **文献标识码** A

doi: 10.3788/LOP53.011404

1 Introduction

The operating temperature of a semiconductor laser (junction temperature) significantly influences the luminous efficiency of the device, its lasing spectra, and lifetime[1-2]. Research on the junction temperature measurement and thermal characteristics of the laser devices is crucial to enhance their efficiency and reliability. Nowadays, the wall plug efficiency of the semiconductor lasers can reach to 50%[3]. However, owing to the non-radiative recombination, free carrier absorption, and ohmic contact, the loss of carrier will make the junction temperature rise. A high working temperature leads to a decreased efficiency, wavelength redshift, and material defects hyperplasia, resulting in reduced reliability and lifetime[4-5]. Thus, the junction temperature is a key factor affecting the laser performance. Thermal resistance is the main parameter to

收稿日期: 2015-08-03; **收到修改稿日期**: 2015-09-04; 网络出版日期: 2015-12-18

基金项目: 国家973计划(2013CB632801)

作者简介: 杨 扬(1987—),男,博士后,主要从事大功率半导体激光器封装、失效分析和可靠性等方面的研究。
E-mail: yangyang.zju@163.com

导师简介: 徐现刚(1964—),男,教授,博士生导师,主要从事半导体光电材料及器件和晶体生长等方面的研究。
E-mail: xuxg@inspur.com

*通信联系人 。E-mail: yangyang.zju@163.com

quantify the cooling capacities of laser devices, which is the ratio of the temperature difference between the laser chip and the heat sink for heat production. Since the main limiting factor on the heat dissipation path is the infiltration and integrity of the solder layer, the output power and reliability of semiconductor laser as well as the sintering quality of the laser chip solder layer should be improved in order to reduce the junction temperature[6].

It is difficult to directly measure the junction temperature. The active layer of the semiconductor laser is located inside the quantum well region, which is in nanometer scale. Generally, a micro- galvanic measurement can only be conducted at the heat sink near the chip, and is unable to detect the chip encapsulated into a shell. As far as the infrared imaging method[7-8] is concerned, it is difficult to accurately detect the junction temperature because of the interference noise of the surrounding infrared radiation, because of which the packaged chip cannot be measured. Since the mutual influence of the electrical-optical-thermal properties in laser, the thermal parameters can be reflected by the electrical or optical testing, i.e, the junction temperature[9]. The forward-voltage method[10-13] is based on the approximately linear relationship between the voltage and the junction temperature. The temperature rise ΔT is obtained by measuring the voltage difference ΔV at different working conditions. The wavelength-shift method[14-15] determines the temperature rise based on the variation of the lasing wavelength. The temperature rise ΔT is indirectly calculated by recording the wavelength redshift $\Delta\lambda$. These two methods for measuring the junction temperature are widely used, but with no comparison.

Notably, by far there is no direct correspondence and analysis between the junction temperature/thermal resistance and the sintering quality of the chips; thus, for the development and manufacture of lasers, it is of limited significance. In order to guide the development and production of laser devices, the study on the relationship between the junction temperature and the package quality is needed. In this paper, we compare the results of the junction temperature of the semiconductor lasers using the forward- voltage and wavelength-shift methods. The comparison and analysis of the junction temperature/thermal-resistance value and solder sintering quality are carried out using a scanning acoustic microscope (SAM). The above-mentioned work provides reference data for the junction temperature/thermal resistance of the semiconductor lasers, which aids the improvement of their packages, cooling, and lifetime.

2 Experimental

The InGaP/InGaAsP quantum-well laser chips are grown by Inspur Huaguang Optoelectronics Co. Ltd. using the metal-organic chemical vapor deposition (MOCVD) method. The strip width is 150 μm, the cavity length is 1.5 mm, and the lasing wavelength is ~808 nm. The P-side of the laser chips are downward-mounted on the AlN ceramic heat sinks coated with gold-tin ($Au_{80}Sn_{20}$) solder, then the heat sinks are sintered on the oxygen-free copper blocks using indium (In) solder. Subsequently, the devices are encapsulated into the package. The schematic diagram for the laser package structure is shown in Fig.1 (a).

The instrument settings are shown in Fig.1 (b) below. The junction temperature and thermal resistance of the laser devices are measured using the LED310 thermoelectric performance analyzer from Zhejiang Everfine Corporation. The devices are fixed onto the temperature control table of the instrument, whose temperature control accuracy is ± 0.1 ℃. The wavelength of the laser is measured using a Japan Yokogawa's AQ6370B spectrometer, with the laser power recorded by a LP- 3B laser power- meter from Beijing Physcience Opto- Electronics Co. Ltd. The sintering quality and void distribution of the solder layer have been analyzed using a German KSI v400E SAM.

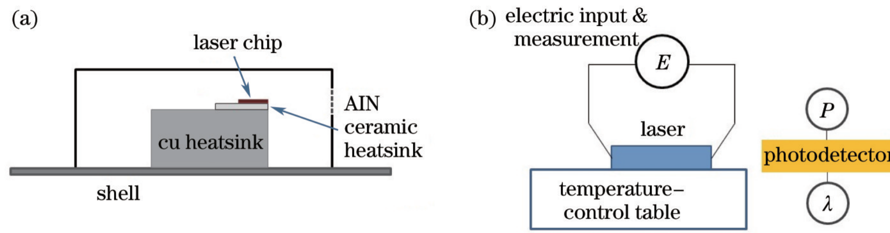

Fig.1 Schematic diagrams for (a) package structure of a laser device and (b) experimental instrument setting

3 Results and discussion

By extensive testing and filtering of the laser devices, we found four types of samples with different junction temperature characteristics. In different batches of the products, these four types of samples appear in different proportions, which should be ascribed to the variations in raw material and workmanship. The representative devices have been tested and analyzed in detail. In the experiment, the test current is 10 mA, and the operating current is 2 A. The test current is only 0.5% of the operating one, whose thermal impact can be negligible. The instrument automatically varies the temperature and measures the forward voltage of the device under 10 mA, the voltage - temperature coefficient K is obtained by linear fitting. Based on the voltage difference and the K-coefficient, the temperature rise ΔT is calculated, resulting in an operating junction temperature. In the same batch of chips, the coefficient K is very close, the standard measurement of the difference is less than 1% of the measured average. The thermal resistance (R) of the laser device is calculated by the formula:

$$R = \frac{\Delta T}{UI - P_{\mathrm{ld}}}, \tag{1}$$

Where U and I are the working voltage and current, respectively. Table 1 shows the operating junction temperature and thermal resistance values of the four typical laser devices using the forward-voltage method. Although the chips are of the same batch, the differences of the junction temperature and thermal resistance between the samples are still considerable. By comparison, we believe that the device A is normal, and that its value can be used as a standard. The junction temperature/thermal resistance value of device B is slightly higher, while that of device C is significantly higher than A and B; the high junction temperature of the device D is mainly due to the low optical power, and the calculated thermal resistance is relatively close to the normal one.

Table 1 Junction temperatures and thermal resistances measured by the forward-voltage method

Sample	Operating voltage /V	Laser power /W	ΔT /℃	R /(℃/W)
A	2.004	1.451	17.61	6.89
B	1.990	1.433	20.05	7.87
C	2.002	1.445	24.98	9.76
D	1.984	1.227	19.50	7.11

At elevated temperatures, the bandgap (E_g) of semiconductor materials shrinks, and thus, the lasing wavelength shows an approximately linear redshift with the temperature rise, i.e., $\Delta\lambda = k \cdot \Delta T$. We have measured the wavelength-shift of the experimental devices with the environmental temperatures. A pulse generator is used to input a pulsed current with a duty ratio of 1% (100 μs, 100 Hz, peak current 1 A). In a working condition with short pulses and a small duty cycle, the thermal effect of the current can be ignored. The measured coefficient between the laser wavelength and the junction temperature could be a standard for determining the junction temperature of laser devices.

After achieving the thermal equilibrium of the laser device and the equipment, we record the lasing wavelength under the pulsed current injection and variable temperatures. The experimental results of three

batches of laser devices are shown in Fig. 2. The laser wavelengths shift with temperatures, exhibiting a good linear relationship. As a result of the same semiconductor material and the active layer structure, the slopes of the curves obtained are almost exactly equal, with a value of 0.23 nm/°C. The different lasing wavelengths are due to the slight difference of the epitaxial conditions.

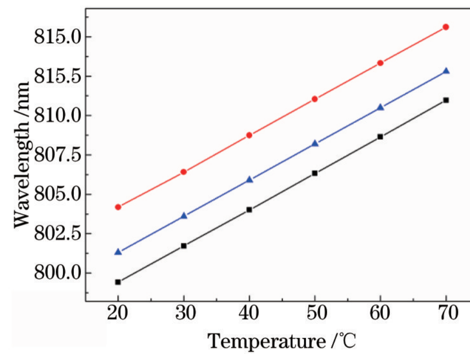

Fig.2 Lasing wavelength shift of laser devices with variable temperatures

The lasing wavelengths of the devices are shown in Table 2; λ_1 is the wavelength recorded under the pulsed current, while λ_2 is that under an operating direct current (DC) current of 2 A. Considering the wavelength shift to the temperature, as shown in Fig.2, the operating temperatures are calculated. The data in these two tables are plotted in Fig.3. As can be seen, the value of the junction temperature obtained from the forward-voltage method is somewhat higher than that measured using the wavelength-shift method, which is about 90% of the former. However, the trend of the junction temperature values of samples obtained by the two methods is the same.

Table 2 Junction temperatures measured by the wavelength-shift method

Sample	λ_1 /nm	λ_2 /nm	ΔT /℃
A	801.92	805.51	15.61
B	802.04	806.20	18.09
C	798.97	804.02	21.96
D	803.88	808.00	17.91

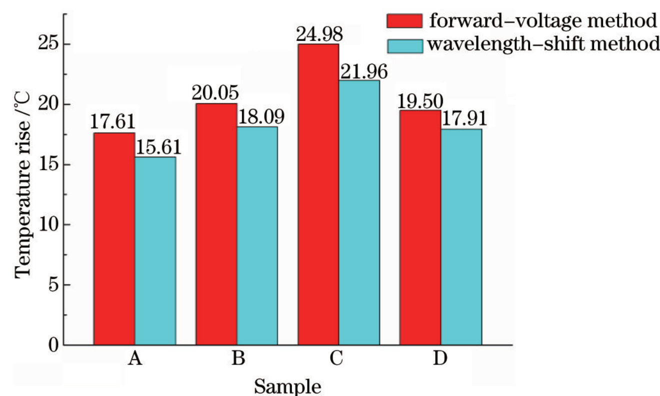

Fig.3 Comparison of laser junction temperature rise using two methods

In this analysis, linear fitting calculation is used. However, due to some non-linear factor, there is a certain deviation. Although the thermal control of the laser device reaches the steady state in the measurements, because of the heat capacity of the overall package and heat dissipation, there may be a certain temperature gradient between the chips and the environment, i.e, the "ambient temperature" of the chips could be somewhat higher than the control temperature of the equipment. The obtained emission peaks envelope several adjacent longitudinal- mode lasing emissions, which have a certain peak width, while the spectrometer records the central position of the entire peak, which is an overall resultant performance of

the electrical-optical-thermal condition in the whole laser resonator. Forward-voltage measurement should be more accurate than the wavelength-shift method. In the electrical measurement, the hysteresis of the voltage-current conversion is quite small, may be of a few s. The obtained temperature data is closer to the actual one[16-17]. Thus, the forward-voltage and wavelength-shift methods are both effective ways to detect the operating junction temperature of lasers, while the forward-voltage method is of higher measurement accuracy, and it also provides more realistic value.

Different junction temperature/thermal resistance values mean that the devices are differentiated on the basis of the ability of heat radiation. In the laser devices, the overall thermal resistance includes all the materials and the contact interfaces on the heat transfer path. Thermal conductivities of copper and AlN ceramics are 400 and 170 W/(m·K), much higher than the solders, so the difference in junction temperatures mainly reflects the sintering quality of the solder layer. The thermal conductivity of the voids in the solder layer is quite low. A high void proportion means a limited radiation path in the solder layer, resulting in a larger thermal resistance and higher junction temperature. In the device structure, the solder layers consist of a 5 μm AuSn solder between the chip and AlN heat sink, and a 12~15 μm In solder between the AlN heat sink and copper block. Considering the thickness, the In solder layer is less likely to contain voids. As the chip area is much smaller than the heat sink, the thin layer of AuSn solder is not only prone to contain voids, but also the voids could result in a higher reduction of the thermal path. In addition, the thermal conductivity of the AuSn alloy [57 W/(m·K)] is less than In [81.6 W/(m·K)]. Thus, we believe that the AuSn solder under the laser chip is a key factor affecting the thermal performance of the laser device, the voids in which will lead to a significant rise in junction temperature/thermal resistance.

The confirmation of the distribution of voids in the solder layer needs microscopic analysis. The sintering conditions of AuSn solder is in general difficult to observe. In order to verify the relationship between the junction-temperature / thermal-resistance and the sintering quality, we use SAM to analyzes the sintering condition of the AuSn solder layer. Acoustic analysis is suitable for most solid materials, which can analyze a layer of material distribution in depth and is extremely sensitive to detect voids. Figure 4 shows the SAM images of the AuSn solder layers under the chips, together with the rise value of the junction-temperatures obtained by forward-voltage method.

Fig.4 SAM images marked with the corresponding junction temperature rise

Both the images of samples A and D are uniform, and the color is almost black, indicating that the solder layers get denser after sintering and have no voids. The image of sample B is uniform, but the color is dark gray, meaning different acoustic impedance is obtained from a dense solid. Thus, in sample B, the whole chip is bonded by the solder, but the alloy sintering reaction is not fully complete, with some existing microdefects. In comparison, in sample C, we find significantly whitish regions under the chip, which represents the presence of larger voids after sintering[18].

Combined with the production experience and the analysis on the surface of the solder after stripping, the relatively high junction temperature/thermal resistance value in sample B should be ascribed to the somewhat poorly sintered AuSn solder layer, which contains microdefects. The cooling efficiency of the heat sink to the environment is reduced, but the whole chip and the heat sink are bonded. The main reason is the

fluctuation of sintering temperature, which could be solved by increasing the equipment stability. In sample C, the high junction temperature/thermal resistance values derived from the significant voids in the AuSn solder layer, especially the large area under the front end of the chip. The voids accumulate the heat generated by the chip, significantly limit the heat dissipation, and increase the operating junction temperature. The formation of the voids is ascribed to the surface contamination on the chip and solder, the uneven composition of the solder, and the skewed fixture when sintering the chip on the solder. Its ratio can be reduced by the screening and protection of the raw material. The results in the SAM images are consistent with the above measurements, which confirm the junction temperature results. The optical power of sample D is only about 85% of the normal sample A, which comes from the lower conversion efficiency of the chip. Although the sintering condition is good, under a similar electrical input power the produced heat is more, resulting in a higher junction temperature, but normal thermal resistance.

Although the production of the above defective devices cannot completely be avoided, the quality of downstream devices could be guaranteed by testing and filtering. The above results confirm the relationship between the junction temperature/thermal resistance and the sintering quality of laser devices. The laser device with poor sintering quality can be sieved, which yields high junction temperature and thermal resistance during the measurement, while the laser device with low efficiency can be filtered out by power measurement. This work provides a basis of reference for the evaluation and sieving of the laser devices by the junction temperature/thermal resistance measurements.

4 Conclusion

The operating junction temperature and thermal resistance of the semiconductor lasers are measured using the forward-voltage and wavelength-shift methods, respectively. The feasibility and reliability of the two methods have been compared. The distribution of the voids in the solder layers is analyzed using SAM, which confirms the reason for the rise in junction temperature/thermal resistance and the correspondence between the junction temperature and sintering quality. This work provides evidence for the measurement of the electrical-optical-thermal properties of the semiconductor lasers, as well as the evaluation of the sintering quality and reliability of the laser devices.

References

1 G I. Ryabtsev, A N Kuzmin, J A. Ges, *et al.*. Thermal properties of high-power In GaAs/AlGaAs laser diodes[J]. Journal of Applied Spectroscopy, 1995, 62(5): 900-902.

2 Jiang Kai, Li Peixu, Shen Yan, *et al.*. 76% maximum wall plug efficiency of 940 nm laser diode with step graded index structure [J]. Chinese J Lasers, 2014, 41(4): 0402003.

蒋 锴, 李沛旭, 沈 燕, 等. 76%光电转换效率梯度渐变折射率结构940 nm半导体激光器[J]. 中国激光, 2014, 41(4): 0402003.

3 G Liu, X J Tang, L J Xu, *et al.*. Fluid-solid coupled heat transfer design numerical study for water cooling CCEPS laser[J]. Chinese J Lasers, 2014, 41(4): 0402004.

刘 刚, 唐晓军, 徐鎏婧, 等. CCEPS激光器水冷设计的流固耦合传热数值研究[J]. 中国激光, 2014, 41(4): 0402004.

4 Z H Tian, C L Sun, J S Cao, *et al.*. Junction temperature measurement of high power diode lasers[J]. Optics and Precision Engineering, 2011, 19(6): 1244-1249.

田振华, 孙成林, 曹军胜, 等. 准连续输出大功率半导体激光器的结温测试[J]. 光学精密工程, 2011, 19(6): 1244-1249.

5 J J Wen, J A Xia. Diode laser pumping structures of solid-state slab lasers[J]. Laser & Optoelectronics Progress, 2007, 44 (4): 44-49.

温姣娟, 夏金安. 固体板条激光器的半导体激光抽运结构[J]. 激光与光电子学进展, 2007, 44(4): 44-49.

6 Y Zhang, R X Yang, Z F An, *et al.*. Influence of cavity length on single emitter semiconductor laser performance[J]. Semiconductor Device, 2013, 38(12): 914-918.

张 勇, 杨瑞霞, 安振峰, 等. 腔长对高功率单管半导体激光器性能的影响[J]. 半导体器件, 2013, 38(12): 914-918.

7 C C Lee, J Park. Temperature measurement of visible light-emitting diodes using nematic liquid crystal thermography with laser illumination[J]. IEEE Photonics Technology Letters, 2004, 16(7): 1706-1708.

8 Z Q Lin, X B Zheng, L Zhang, *et al*.. Calibration of infrared radiation based on cryogenic radiometer[J]. Laser & Optoelectronics Progress, 2007, 44(4): 62-67.

林志强, 郑小兵, 张磊, 等. 基于低温辐射计的红外辐射定标方法[J]. 激光与光电子学进展, 2007, 44(4): 62-67

9 X Liu, T Li, G G Lu, *et al*.. Research on electric derivatives and reliability of semiconductor lasers[J]. Laser & Optoelectronics Progress, 2015, 52(4): 041404.

刘　夏, 李　特, 罗国光, 等. 半导体激光器电导数及其可靠性的研究[J]. 激光与光电子学进展, 2015, 52(4): 041404.

10 H Y Ryu, K H Ha, J H Chae, *et al*.. Measurement of junction temperature in GaN-based laser diodes using voltage-temperature characteristics[J]. Applied Physics Letters, 2005, 87(9): 093506.

11 X Fei, K Y Qian, Y Luo. Junction temperature measurement and luminous properties research of high-power LED[J]. Journal of Optoelectronics·Laser, 2008, 19(3): 289-292.

费　翔, 钱可元, 罗　毅. 大功率LED结温测量及发光特性研究[J]. 光电子·激光, 2008, 19(3): 289-292.

12 J H Han, S W Park. Theoretical and experimental study on junction temperature of packaged Fabry-Perot laser diode[J]. IEEE Transactions on Device & Materials Reliability, 2004, 4(2): 292-294.

13 Z J Zhang, Y Liu, X H Fu, *et al*.. Analysis on overall thermal resistance of laser diode beam combined modules[J]. Chinese J Lasers, 2012, 39(4): 0402010.

张志军, 刘　云, 付喜宏, 等. 激光二极管合束模块整体散热热阻分析[J]. 中国激光, 2012, 39(4): 0402010.

14 M K Su, G Q Ni, F Zuo. Frequency bath ochromic shift used for testing the thermal resistors of laser diodes[J]. Opto-Electronic Engineering, 2007, 34(5): 48-51.

苏美开, 倪国强, 左　昉. 频率红移法用于激光二极管热阻测量[J]. 光电工程, 2007, 34(5): 48-510.

15 X K Hou, L Q Zhang, S L Zhang, *et al*.. Precise thermal simulation module for DFB laser sub-assembly with transistor outline package[J]. Chinese J Lasers, 2013, 40(10): 1002006.

侯小珂, 张丽卿, 张胜利, 等. 一种精确的同轴封装DFB激光器组件的热学模型[J]. 中国激光, 2013, 40(10): 1002006.

16 Y Xi, E F Schubert. Junction-temperature measurement in GaN ultraviolet light-emitting diodes using diode forward voltage method[J]. Applied Physics Letters, 2004, 85(12): 2163-2165.

17 D Luo, W L Guo, C Xu, *et al*.. Junction temperature measurement of semiconductor laser diode[J]. Semiconductor Optoelectronics, 2007, 28(2): 183-190.

罗　丹, 郭伟玲, 徐　晨, 等. 半导体激光器结温测试研究[J]. 半导体光电, 2007, 28(2): 183-190.

18 J W Wang, Z B Yuan, Y X Zhang, *et al*.. Study on the mechanisms of spectral broadening in high power semiconductor laser arrays[J]. Chinese J Lasers, 2010, 37(1): 92-99.

王警卫, 袁振邦, 张彦鑫, 等. 大功率半导体激光器阵列光谱展宽机理研究[J]. 中国激光, 2010, 1: 92-99.

栏目编辑： 宋梅梅